

**ASYMMETRY INDUCED HEAT CURRENT
RECTIFICATION AND MAGNIFICATION IN
BOUNDARY DRIVEN SPIN AND FERMIONIC
SYSTEMS**

VIPUL UPADHYAY



DEPARTMENT OF PHYSICS

INDIAN INSTITUTE OF TECHNOLOGY DELHI

JUNE 2024

© Indian Institute of Technology Delhi (IITD), New Delhi, 2024

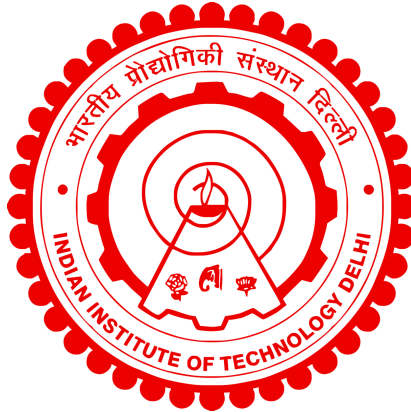
**ASYMMETRY INDUCED HEAT CURRENT
RECTIFICATION AND MAGNIFICATION IN
BOUNDARY DRIVEN SPIN AND FERMIONIC
SYSTEMS**

**VIPUL UPADHYAY
2018PHZ8435**

Department of Physics

Submitted

in partial fulfillment of the requirements of the degree of Doctor of Philosophy
to the



INDIAN INSTITUTE OF TECHNOLOGY DELHI

JUNE 2024

*Dedicated to my loving parents, Mr. Pradeep Kumar
Upadhyay and Mrs. Damyanti Upadhyay*

Certificate

This is to certify that the thesis entitled “**Asymmetry induced heat current rectification and magnification in boundary driven spin and fermionic systems**”, submitted by **Vipul Upadhyay** to the Department of Physics, Indian Institute of Technology Delhi, for the award of the degree of **Doctor of Philosophy** in Physics, is a record of the original, bona fide research work carried out by him under my supervision and guidance. The thesis has reached the standards fulfilling the requirements of the regulations related to the award of the degree.

The results contained in this thesis have not been submitted in part or in full to any other University or Institute for the award of any degree or diploma to the best of my knowledge.



28/06/2024

Prof. Rahul Marathe

Associate Professor

Department of Physics

Indian Institute of Technology Delhi

New Delhi - 110016, India

Acknowledgements

I would begin the acknowledgements by thanking my parents, Mr. Pradeep Kumar Upadhyay and Mrs. Damyanti Upadhyay, for all the love and support they have provided during my academic journey. They along with my two amazing sisters Vidhi and Jagrati, have always encouraged me to be an independent thinker and have constantly motivated me to pursue my academic interests. I owe most of my curiosities in science to the encouraging upbringing that they have provided.

I am highly indebted to my thesis supervisor, Prof. Rahul Marathe, for the wonderful experience I had during my time as a Ph.D. research scholar at IIT, Delhi. He has been an exemplary supervisor, excelling not only in academic supervision but also being a person whose individual qualities outside work are very inspiring and worth replicating. He has always amazed me with his penetrative thinking and his ability to ask the right questions. He granted me total academic freedom in the diverse research problems we explored, displaying unwavering patience when I encountered challenges. I owe most of the intuition that I developed in non-equilibrium dynamics to the years of collaboration with him.

I also want to thank my frequent collaborators cum teachers, Dr. Muhammad Tahir Naseem and Prof. Özgür Müstecaplıoğlu of Koç University, Istanbul, Türkiye. They have always been so kind and much of what I understand about Markovian Quantum Master Equations is due to the numerous conversations I had with them. A special thanks to Dr. Juzar Thingna at the American Physical Society for teaching me the significance of each approximation that goes inside deriving these equations microscopically.

I express my gratitude to my lab members and friends Rita, Mintu, Yatin sir, Yasir bhai, Vikky, Simmi, Roshan, Vikas, Monojit and Partho, for providing a familial environment inside the lab. It was a great pleasure to have such empathetic people around, always ready for providing help in professional as well as personal matters.

Lastly, I thank my friends. Getting a Ph.D. is a long journey, it would have been impossible to cover this entire journey without the love and support of each one of them. I can't imagine my Ph.D. life without Deepika, Ravindra, Vishal, Lalit, Sharad, Viresh, Arun bhai and many more who have made Delhi my primary home during this time. I will always cherish the many memories we made at the little den that we have in Jia Sarai.

Abstract

The broader aim of this thesis is to enhance our understanding of heat current transport in mesoscopic and nanoscopic quantum systems. To accomplish this, we investigate how structural asymmetry influences steady state thermal transport in such small scaled systems. We divide our studies into two sub-classes. One subclass deals with construction of thermal devices for better manipulation of heat currents and the other deals with the investigation of anomalous transport phenomenon due to asymmetry. We employ spin and fermionic lattice models for studying these sub-classes and the analysis is done using the quantum Markovian master equations.

Specifically, for the first subclass we study the construction of thermal diodes which are the most fundamental small scaled devices needed to manipulate heat currents. In the initial part of this subclass, we study the heat current rectification effects in a two qubit (spin-1/2 particle) setup. These two qubits interact with each other via the Dzyaloshinskii-Moriya (DM) interaction and are coupled to two separate heat baths. Off-resonant magnetic field is applied on these spins and it is observed that this inhomogeneous magnetic field serves as the asymmetry required for inducing the heat rectification. For the later segment of this subclass, we study the potential of a heat diode to distinguish different topological phases of the Su-Schrieffer-Heeger (SSH) model. This study explores in detail the role of heat transport as a potential indicator of topological phase transition in the SSH model, and demonstrates how the efficiency of the diode can be exploited as the quantity used to distinguish between the different topological phases.

In the second subclass, we study an interesting transport phenomena called Current Magnification (CM) or Current Circulation (CC). The investigation of this phenomenon requires placing a multi-branched system between the two heat baths. CM occurs when in one of the system branches, the local heat current is larger than the total heat current, and in the other branch, the heat current flows in opposite direction of the thermal gradient. This is necessary for conserving the total current at the junction. Similar to our treatment of heat rectification, we initiate this subclass by studying a small quantum spin setup. Here, we establish that the geometrical asymmetry of having unequal number of spins in different system branches is enough to generate CM. Analysing this system in more detail, we realise that CM usually occurs near the point of intersection of two otherwise non-degenerate energy levels. We call this point the Additional Energy Degeneracy Point

(AEDP). Next, we examine CM in a quadratic fermionic network and provide analytical proof of its possible presence near AEDP. Subsequently, we apply this idea to different fermionic models with quadratic Hamiltonians and verify the relationship between CM and AEDP.

In our efforts while examining both these subclasses, it becomes apparent that while asymmetry is a crucial condition for observing heat current rectification and magnification, it alone is insufficient for either of these phenomena, and other complementary properties like anharmonicity or AEDP in the system are required.

शोध सार

इस थीसिस का मुख्य उद्देश्य मेसोस्कोपिक और नैनोस्कोपिक क्वांटम तंत्रों में ऊष्मा धारा परिवहन की हमारी समझ का विस्तार करना है। इस लक्ष्य को प्राप्त करने के लिए, हम इन लघु-स्तरीय तंत्रों में स्थिर-अवस्था ऊष्मा परिवहन पर संरचनात्मक असममिति के प्रभाव की जांच करते हैं। हम अपने अध्ययन को दो भागों में विभाजित करते हैं। एक भाग ऊष्मा धाराओं को बेहतर तरीके से नियंत्रित करने के लिए ऊष्मा उपकरणों के निर्माण पर केंद्रित है, और दूसरा असममिति के परिणामस्वरूप होने वाली असामान्य ऊष्मा परिवहन घटनाओं का अन्वेषण करता है। हम इन भागों का अध्ययन करने के लिए स्पिन और फर्मियोनिक लैटिस मॉडल का उपयोग करते हैं, एवं विश्लेषण के लिए क्वांटम मार्कोवियन मास्टर समीकरण का प्रयोग करते हैं।

विशेष रूप से पहले भाग के लिए हम ऊष्मा डायोड के निर्माण का अध्ययन करते हैं। यह ऊष्मा धाराओं को प्रबंधित करने के लिए सबसे मौलिक छोटे पैमाने के उपकरण हैं। इस उप-वर्ग के प्रारंभिक भाग में, हम एक दो क्यूबिट (स्पिन-1/2) तंत्र में ऊष्मा धाराओं के प्रवाह का अध्ययन करते हैं। ये दो क्यूबिट अलग-अलग तापमान के ऊष्मा स्नानों से जुड़े हैं, एवं एक दूसरे पर इज़्यालोशिन्स्की-मोरिया (डी. एम.) प्रभाव के द्वारा असर डालते हैं। इन दो स्पिन पर अलग अलग चुंबकीय क्षेत्र डाला जाता है जिस कारण ऊष्मा धारा के प्रवाह में असममिति आती है, जिसके परिणामस्वरूप ऊष्मा डायोड का निर्माण किया जाता है। इस वर्ग के आगे के हिस्से में, हम एक ऐसे ऊष्मा डायोड की संभावना का अध्ययन करते हैं जो सु-श्रीफर-हीगर (एस. एस. एच.) मॉडल के विभिन्न टॉपोलॉजिकल चरणों को अलग करने के लिए उपयुक्त है। यह अध्ययन एस. एस. एच. मॉडल में ऊष्मा परिवहन की भूमिका को विस्तार से जांचता है, और सिद्ध करता है कि ऊष्मा परिवहन से भिन्न टॉपोलॉजिकल चरणों को चिन्हित किया जा सकता है।

दूसरे भाग में, हम एक रोचक परिवहन प्रक्रिया का अध्ययन करते हैं, जिसे 'करंट मैग्निफिकेशन' (सी. एम.) या 'करंट सर्कुलेशन' (सी.सी.) कहा जाता है। इस अन्वेषण के लिए, हमें दो ऊष्मा स्नानों के बीच एक बहु शाखायुक्त तन्त्र रखना होता है। सी.एम. तब होता है जब एक शाखा में स्थानीय ऊष्मा धारा का परिमाण कुल ऊष्मा धारा के परिमाण से अधिक हो जाता है। परिणामस्वरूप दूसरी शाखा में, ऊष्मा धारा का प्रवाह तापमान पक्ष की विपरीत दिशा में होता है। यह कुल धारा को संगम पर संरक्षित रखने के लिए आवश्यक होता है।

हम पिछले भाग की तरह ही, इस खंड की शुरुआत एक छोटे क्वांटम स्पिन तंत्र का अध्ययन करके करते हैं। यहाँ, हम सिद्ध करते हैं कि शाखाओं में असमान संख्या के स्पिनो की ज्यामितिक असममिति सी. एम. उत्पन्न करने के लिए पर्याप्त है। इस प्रणाली को अधिक विस्तृत रूप से विश्लेषित करते हुए, हम पाते हैं कि सी.एम. आमतौर पर दो गैर-समान ऊर्जा स्तरों के संपर्क के बिंदु के पास होता है। हम इस बिंदु को अतिरिक्त ऊर्जा समानता बिंदु (ए.इ.डी.पी.) कहते हैं। इस

अवलोकन को ध्यान में रखते हुए, आगे हम एक क्वाड्रटिक फर्मियोनिक संजाल में सी.एम. का अध्ययन करते हैं। यहाँ हम सी.एम. और ए.इ.डी.पी. के बीच के संबंध की विश्लेषणात्मक पुष्टि करते हैं, एवं इस प्रकल्पना की अलग-अलग क्वांटम तंत्रों में जांच करते हैं।

अंततः हमारे प्रयासों के दौरान यह स्पष्ट होता है कि असममिता ऊष्मा डायोड के निर्माण एवं सी.एम. के अवलोकन के लिए एक महत्वपूर्ण शर्त है। लेकिन केवल यह अपने आप में पर्याप्त नहीं है, और अन्य सहायक गुणात्मक गुणों जैसे कि अन्हारमोनिसिटी या ए.इ.डी.पी. की भी आवश्यकता होती है।

Contents

Certificate	i
Acknowledgements	iii
Abstract	v
Contents	ix
List of Figures	xiii
Abbreviations	xix
Symbols	xxi
1 Introduction	1
1.1 Objectives of the Thesis	5
1.1.1 Current Rectification	6
1.1.2 Current Magnification (CM) or Current Circulation (CC)	8
1.2 Thesis Organisation	9
2 Methodology: Markovian Quantum Master Equations	13
2.1 Lindblad Master Equation	20
2.1.1 Global Lindblad Master Equation	21
2.1.2 Local Lindblad Master Equation	24
2.2 Heat Current Definitions	25
2.2.1 Global Heat Current	25
2.2.2 Local Heat Current	26
2.3 Experimental studies and typical parameter ranges	28

3	Heat rectification by off-resonant qubits coupled via Dzyaloshinskii-Moriya (DM) interaction	31
3.1	Introduction	31
3.2	The Model	33
3.3	Master Equation	35
3.4	Results	39
3.4.1	Heat flow analysis	40
3.5	Heat rectification	44
3.5.1	Effect of Anisotropy Field Direction	49
3.6	Quantumness of correlations and rectification	50
3.7	Summary	54
4	Thermal diode as a topological phase identifier in the Su–Schrieffer–Heeger (SSH) model	57
4.1	Introduction	57
4.2	The SSH Model	59
4.2.1	System eigenvalues and eigenvectors	61
4.3	Master equation and heat flow	62
4.4	Results	64
4.5	Heat Current Expression	66
4.5.1	Heat current with system size	68
4.6	Effective temperature and steady state density matrix	71
4.6.1	Thermodynamics of bulk and edge contributions	73
4.7	Heat diode with bosonic baths	75
4.7.1	Heat rectification	76
4.7.2	Diode with a few fermionic sites	78
4.8	Summary	80
5	Current Magnification due to number asymmetry in classical and quantum spin networks	83
5.1	Introduction	83
5.2	Model and Classical Analysis	84
5.2.1	Time evolution dynamics	86
5.2.2	Heat Current Definitions	87
5.2.3	Information about Methodology	88
5.2.4	Q2R dynamics with symmetric upper and lower branch interaction strength	89
5.2.5	Q2R dynamics with asymmetric upper and lower branch interaction strength	93
5.2.6	Possible Physical Mechanism	96
5.2.7	CCA Model	98
5.3	Quantum Analysis	101

5.3.1	The model	101
5.3.2	Master Equation	103
5.3.3	Definitions	105
5.3.4	Information about numerical methodology	107
5.3.5	Results	108
5.4	Summary	112
6	Current Magnification near additional energy degeneracy points (AEDP) in quadratic Fermionic networks	113
6.1	Introduction	113
6.2	System Hamiltonian and Master Equation	114
6.2.1	Master equation	115
6.2.2	Correlation Matrix Master equation	116
6.3	Solving The Master Equation for diagonalisable \hat{A}	118
6.3.1	Expression for Currents	119
6.3.2	Perturbation theory	119
6.4	Application to the SSH Model	123
6.4.1	Particle and Heat Current definition	123
6.4.2	Even N Results	126
6.4.3	Odd N	128
6.4.4	Plausible Physical mechanism behind circulation	131
6.5	Model with unequal upper and lower branch hopping strengths	133
6.6	Summary	135
7	Conclusions and Future Prospective	137
7.1	Future Prospective: A proposal on Parameter-induced current anomalies (PICAs) and their Applications to Metrology	139
	Bibliography	145
	Appendix A: Heat rectification by off-resonant qubits coupled via DM interaction	165
A.1	Heat Current Expression Derivation	165
	Appendix B: Heat diode as a topological phase identifier in the SSH model	167
B.1	Master Equation Derivation	167
B.2	Heat Current Expression Derivation	169
B.3	Heat Current for different bath spectrum functions	170
	Appendix C: CM near AEDP in quadratic Fermionic networks	171

C.1	Local Master Equation Derivation	171
C.2	Correlation Matrix Master Equation	172
C.3	Correlation matrix for quadratic Bosonic systems	173
	List of Publications	175
	Curriculum Vitae	177

List of Figures

- 1.1 Schematic of a boundary driven thermal system. The system is kept between two heat baths at different temperatures T_L and T_R . 2
- 1.2 A schematic diagram showing the configurations corresponding to the two biases of a thermal diode with $T_L > T_R$. The depicted diode prefers the direction of flow from left to right and $I_F > I_R$. The rectification factor is proportional to the difference in the currents obtained via the two different biases. 6
- 1.3 A typical configuration for studying CM. The two baths are connected by a multi-branched system. The total current (I_L) divides in the branch and three possible ways of heat transfer are possible. Symmetric or parallel transport in the branches, clockwise current circulation or anti-clockwise current circulation 8
- 2.1 A cartoon demonstrating an open quantum system. 13
- 3.1 A schematic of the model consisting of two qubits coupled by the Dzyaloshinskii Moriya (DM) interaction with on-site (local) magnetic fields. Each qubit is attached to its own local bath. 33
- 3.2 Energy transitions induced by left (solid lines) and right (dashed lines) baths for weakly coupled (a) off-resonant qubits, and (b) for nearly-resonant qubits. 35
- 3.3 Steady-state right heat bath current I_R as a function of temperature T and coupling strength g . (a) Comparison between the analytical (blue solid line) and numerical (red circles) results of heat current I_R evaluated via Eq. (3.25) and Eq. (3.24), respectively. We take $T_{\text{ref}} = 1$ being reference temperature, and $T_R \equiv T, T_L = T_{\text{ref}}$ describes forward-biased configuration. (b) Forward-biased (blue solid line) and reverse-biased (red dashed line) heat current I_R , where reverse-biased (RB) configuration is described by $T_R = T_{\text{ref}}, T_L \equiv T$. (c) Forward-biased (FB) heat current for $g=0.01$ (blue solid line), $g=0.1$ (red dashed line), $g=1.0$ (green dotted line), and (d) I_R as a function of DM interaction strength g for RB current (blue solid line), and FB current (red dashed line). In both cases, we consider $T_{\text{High}} = 10$, and $T_{\text{Low}} = 1$. Rest of the parameters are given as: $\omega_L = 1$, $\omega_R = 0.1$, $\kappa = 0.0001$, and $g = 0.01$. All the parameters are scaled with the left qubit frequency $\omega_L = 2\pi \times 10$ GHz. 42

- 3.4 Examples of the procedure that transfer heat between the baths for the weakly interacting resonant qubits $\omega_L = \omega_R = \omega \gg g$. The separation between energy levels $|2\rangle$, and $|3\rangle$ becomes $4g$, and ω_{\pm} transitions reduce to $\omega \pm 2g$. Solid, and dashed arrows indicate the transitions induced by the left and right baths, respectively, and the thickness of the arrows reflects the magnitudes of the decay rates between the states. In addition, dot-dashed arrows point the direction of the heat flow. For resonant qubits, all transition rates become symmetrical under the change in temperature bias due to which rectification becomes zero. 43
- 3.5 Variation of rectification (\mathcal{R}) with temperature T (top row) for **(a)** $\omega_R=0.005$ (blue solid line), $\omega_R=0.05$ (red dashed line), $\omega_R=0.4$ (green dotted line), $\omega_R=0.8$ (black dot-dashed line), for **(b)** $g=0.005$ (blue solid line), $g=0.05$ (red dashed line), $g=0.4$ (green dotted line), $g=0.8$ (black dot-dashed line). Variation of \mathcal{R} with g for **(c)** $\omega_R=0.005$ (blue solid line), $\omega_R=0.05$ (red dashed line), $\omega_R=0.4$ (green dotted line), $\omega_R=0.8$ (black dot-dashed line) with $T_R = 10$ and $T_L = 1$. **(d)** Shows the direction of rectification can be controlled by detuning ω_D . Here, $\omega_D > 0$ (blue solid line), $\omega_D < 0$ (red dashed line). For all the cases, the values of parameters if not otherwise specified are $\omega_L = T_{\text{ref}} = 1$, $\omega_R = 0.1$, $g = 0.01$, and $\kappa = 0.0001$. 47
- 3.6 **(a)** Parametric curve between rectification (\mathcal{R}) and I_R for $\omega_R=0.01$ (blue solid line), $\omega_R=0.05$ (red dashed line), $\omega_R=0.1$ (green dotted line), $\omega_R=0.5$ (black dot-dashed line) with $T_R = 10$, $T_L = 1$. Variation of I_R with T for **(b)** DM along x (blue solid line), along y (red dashed line), along z (green dotted line). Variation of \mathcal{R} with T for **(c)** DM along x (blue solid line), along y (red dashed line), along z (green dotted line). **(d)** Changing the sign of \mathcal{R} by exchange of qubit frequencies for DM along x (blue solid line, green dotted line) and for DM along y (red dashed line, black dot-dashed line). For all the cases the values of parameters if not otherwise specified are $\omega_R = 0.1$, $g = 0.05$, $\kappa = 0.0001$, $\omega_L = 1$, $T_{\text{ref}} = 1$. 49
- 3.7 **(a)** Variation of rectification and coherence with g for $T_R = 5$ (blue solid line for \mathcal{R}) and (green dotted line for coherence) and $T_R = 10$ (red dashed line for \mathcal{R}) and (black dot-dashed line for coherence) and **(b)** Variation of rectification and concurrence with g for $T_R=5$ (blue solid line for \mathcal{R}) and (green dotted line for $C(\rho_{\text{ss}})$) and $T_R=10$ (red dashed line for \mathcal{R}) and (black dot-dashed line $C(\rho_{\text{ss}})$). The values of the parameters are $\omega_R = 0.1$, $g = 0.05$, $\kappa = 0.0001$, $\omega_L = 1$, $T_{\text{ref}} = 1$. 53
- 3.8 **(a)** Variation of rectification \mathcal{R} and asymmetry in the coherences \mathcal{A} as a function of g for $T_{\text{high}} = 5$ (blue solid line for \mathcal{R}) and (green dotted line for \mathcal{A}) and $T_{\text{high}} = 10$ (red dashed line for \mathcal{R}) and (black dot-dashed line \mathcal{A}). Parameters: $\kappa = 0.0001$, $\omega_L = 1$, and $\omega_R = 0.01$. 54

- 4.1 Schematic of the model system. A single SSH chain is connected at left and right ends to two heat baths at temperature T_L and T_R respectively. Double and single bonds signify the relative hopping strengths between sites with double bonds having larger hopping strength than the single bond. 60
- 4.2 **(a)** Energy spectrum with δ . Variation of absolute value of wavefunction at site n for **(b)** near zero as well as non-zero energy states, **(c)** near zero energy states for various δ , (inset) variation of first and last component of eigenvector of a typical non-zero energy mode with δ , **(d)** Variation of heat current with δ for various t 's, **(e)** variation of transmission coefficients for all the non-zero energy modes with δ and **(f)** variation of the curvature of the heat current with δ . For all the case, if not specified otherwise, the values of the parameters are $N = 200, t = 1, T_L = 1, T_R = 0.1, \delta = 0.2, \kappa_L = 0.1, \kappa_R = 0.1$. 65
- 4.3 Variation of heat current with N for **(a)** Topological Phase, **(b)** Trivial phase. **(c)** Comparison of fitting quality of F_1 and F_2 for variation of heat current with N for topological and trivial (inset) phase. **(d)** Variation of edge and bulk current with δ . The edge current in fit F_2 has been scaled by a factor of ' $\frac{1}{50}$ ', for visual convenience. All the fits are done for data in the range $N = \{6, 50\}$. 69
- 4.4 **(a)** Variation of the effective temperature spectrum with δ . The near-zero energy mode effective temperature is also shown for various system sizes N . **(b)** Variation of effective temperature with energy E for the Topological Phase. Variation of edge and bulk contribution with δ for **(c)** entropy S and **(d)** specific heat C_T . 73
- 4.5 Variation of left and right current with **(a)** δ , **(b)** χ , variation of rectification with **(c)** δ , **(d)** χ , **(e)** system size N and **(f)** Variation of edge and bulk contribution to rectification with δ . If not specified otherwise $T_R = 0.1, \chi = -0.5, \delta = 0$. If the figures have empty legend titles, it signifies that we are showing both the left to right current and right to left current on exchanging temperatures for the same value of other parameters. The sign of current is positive for left to right current and vice versa. This means that (blue continuous line) and (green dotted line) represent the left to right currents and (red dashed line) and (black dot-dashed line) represent the right to left currents. 77
- 4.6 **(a)** Variation of left and right current with Temperature T for trivial and topological phase, **(b)** Variation of Rectification with Temperature T , **(c)** Variation of difference between rectification in topological phase and trivial phase ($\Delta\mathcal{R}$) with T . Contour plots showing variation of $\Delta\mathcal{R}$ with **(d)** N, T , **(e)** χ, T and **(f)** δ, T . While doing the variations, temperature of one bath is fixed at ' $T_L(T_R) = 0.1$ '. The parameters if not otherwise specified are ' $\chi = -0.5, N = 10$ and $\delta = 0.2$ '. 79
- 5.1 Schematic representation of the model system 84

- 5.2 Illustration of the model system consisting of 3 spins with $N_U = 1$ and $N_D = 0$. 89
- 5.3 **(a)** Comparison of total current (I_L) between analytical, numerical and simulation results for the 3 spin system with $N_U = 1$, $N_D = 0$, **(b)** Variation of Heat Currents (I) with T_L for $N_U = 1$, $N_D = 0$, **(c)** Variation of I_L with T_L for a 8 spin system but with different branch spin distributions, **(d)** Variation of Heat Currents (I) with N_U for $N_D = 4$, $T_L = 2$, $T_R = 0.1$. For all the cases unless otherwise specified, we use $T_R = 1$, $J = 1$. 92
- 5.4 Variation of Heat Currents (I) with **(a)** T_L , with **(b)** T_L for $N_D = 2$, $N_U = 3$, with **(c)** T_R , with **(d)** J_2 , with **(e)** N_U for $N_D = 4$ and **(f)** Variation of Heat Currents (I) and $\langle \sigma_2 \sigma_3 \rangle$ with T_L . For all the cases, unless otherwise specified we use $J_1 = 2$, $T_L = 2$, $T_R = 0.1$, $J_2 = 1.9$, $N_D = 3$, $N_U = 2$. In all the figures where multiple regions of current circulation directions are present, we use green, gray and yellow background colors to indicate clockwise, parallel and anticlockwise circulating currents respectively. For all other cases, we use a white background. 94
- 5.5 Example of a process which result in the transfer of energy $2(J_1 - J_2)$ from left bath to the right bath. 96
- 5.6 Variation of Heat Currents (I) with **(a)** T_L , with **(b)** J_2 for the system shown in Fig. 5.5 with $N_D = 1$, $N_U = 1$, For all the cases, unless otherwise specified we use $J_1 = 2$, $T_L = 2$, $T_R = 0.1$, $J_2 = 1.9$. 97
- 5.7 Variation of Heat Currents (I) for the CCA model with **(a)** T_L for $J_1 = J_2 = 1$, with **(b)** T_L , with **(c)** T_R and **(d)** with μ . For all the cases unless otherwise specified $J_1 = 2$, $T_L = 2$, $T_R = 0.1$, $J_2 = 1$, $N_D = 3$, $N_U = 2$ and $\mu = 4$. 100
- 5.8 Illustration of the Quantum Spin system consisting of 5 spins with $N_U = 2$ and $N_D = 1$. 102
- 5.9 Variation of Heat Currents (I) with the asymmetry parameter Δ for **(a)** for setup $5(3 \uparrow 2 \downarrow)$ **(b)** for setup $5(2 \uparrow 3 \downarrow)$, **(c)** for a 6 spin system with setup $6(4 \uparrow 2 \downarrow)$ with $N_U = 3$, $N_D = 1$ and **(d)** Variation of Heat Currents (I), correlation and concurrence between spins 2 and 3 with T_L for $\Delta = 2.1$. For all the cases unless otherwise specified we work with the setup $5(3 \uparrow 2 \downarrow)$ and $T_L = 2$, $T_R = 1$, $J = 1$. In **(d)** we scale the correlation and concurrence by a factor 0.2 for the visual convenience. 108
- 5.10 **(a)** Variation of energy levels with Δ , **(b)** Variation of occupation probability (P) with Δ , **(c)** Variation of individual spin magnetisation (M_k) with Δ , **(d)** Variation of ergotropy (ϵ) with Δ , Variation of **(e)** energy levels and **(f)** currents for a larger range of asymmetry parameter Δ . Note that only the magnitude of currents are considered for the log plot in **(f)** but the background colors for parallel, clockwise or anticlockwise circulating currents are kept. For all the cases unless otherwise specified, we work with the setup $5(3 \uparrow 2 \downarrow)$ and $T_L = 2$, $T_R = 1$, $J = 1$. 110

- 6.1 Variation of the function defined in eq. (6.29) with ΔE for various values of **(a)** a, b and **(b)** $E^{(1)} = c$. The default values of parameters are $a = 0.1, b = 0.1, E^{(1)} = c = 0.01$ 121
- 6.2 Schematic diagram of **(a)** SSH model with even N and **(b)** SSH model with odd N with periodic boundary condition. 122
- 6.3 **(a)** Variation of energy Spectrum of the SSH model with δ , variation of particle currents with δ for **(b)** $N_U = N_D = 9$, **(c)** $N_U \neq N_D$. The current 'JP_U' here is the perturbation theory current. **(d)** Variation of max circulating current with N_U . The maximum value of J_C is taken between the range of $\delta \in \{-0.02, 0.02\}$ with one step length of 0.001. **(e)** Variation of energy Spectrum of the SSH model with δ for $N = 18$ and variation of particle currents with δ for **(b)** $N_U = 10, N_D = 6$. If not specified otherwise, $N_U = 10, N_D = 8, T_L = 1, T_R = 0.1, \kappa_{1(N_U+2)} = 0.1, \Omega = 1$. In all figures where multiple regions of CM directions are present, we use green, gray, and yellow background colors to indicate clockwise, parallel, and anticlockwise circulating currents, respectively. For all other cases, we use a white background. 126
- 6.4 **(a)** Variation of energy Spectrum of the SSH model with δ for odd number of fermionic sites, **(b)** Variation of heat currents with δ , **(c)** Variation of particle currents with δ and **(d)** Variation of max circulating current with N_U , Variation of average occupancy at all sites with δ for a system with **(e)** $N_U = 10, N_D = 8$ and **(f)** $N_U = 10, N_D = 6$ If not specified otherwise, $N_U = 10, N_D = 9$. 129
- 6.5 Possible current cycle in a 5-site system resulting in the transfer of 1 particle from left bath to right bath and circulation of a particle in the clockwise direction within the branches. 131
- 6.6 Model with unequal hopping strength in upper and lower branch 133
- 6.7 **(a)** Variation of energy Spectrum of the asymmetric model with δ , **(b)** Variation of heat currents with δ , **(c)** Variation of up branch heat and particle currents with δ and **(d)** Variation of max circulating currents with N_U . If not specified otherwise, $N_U = 10, N_D = 10$ 134
- 7.1 A diagram illustrating **(a)** additional energy degeneracy accompanied by **[(b) and (c)]** two possible instances of anomalous current (I) behaviour, characterized by the parameter ' α '. 140
- B.3.1 **(a)** Variation of heat current with δ for various bath spectrum functions and **(b)** variation of the curvature of the heat current with δ . For all the case, if not specified otherwise, the values of the parameters are $N = 200, t = 2, T_L = 1, T_R = 0.1, \delta = 0.2, \kappa_L = 0.1, \kappa_R = 0.1$. 170

Abbreviations

DM	D zyaloshinskii- M oriya
SSH	Su - S chrieffer- H eeger
CM	C urrent M agnification
CC	C urrent C irculation
AEDP	A dditional E nergy D egeneracy P oint
R.B.T.	R ight B ath T erms
H.C.	H ermitian- C onjugate

Symbols

k_B	Boltzmann Constant
\hbar	Reduced Planck's constant
\hat{H}_T	Total System Hamiltonian
\hat{H}_S	Hamiltonian of the system of interest
\hat{H}_B	Bath Hamiltonian
$\hat{\rho}, \hat{\rho}_S$	Density matrix of the system of interest
$\hat{\rho}_B$	Density matrix of the Bath
$\hat{\rho}_T$	Density matrix of the total system (System + Bath)
$\mathcal{D}_i[\hat{\rho}]$	i -th Dissipator
$\mathcal{D}_i(\hat{A})[\hat{\rho}]$	Lindblad Dissipator with operator \hat{A}
$\mathcal{L}_L[\hat{\rho}]$	Left Liouville Superoperator
$\mathcal{L}_R[\hat{\rho}]$	Right Liouville Superoperator
$I_{L(R)}$	Heat current flowing out of left (right) bath
\mathcal{R}	Heat Rectification
$\hat{\sigma}_j^i$	i -th Pauli matrix corresponding to j -th spin
$C(\rho_{i,j})$	Concurrence between spins i and j